Cancer Science

WILEY

Cancer Science

ORIGINAL ARTICLE OPEN ACCESS

High Antigenicity for T_{reg} Cells Confers Resistance to PD-1 Blockade Therapy via High PD-1 Expression in T_{reg} Cells

Hiroaki Matsuura[1,2] | Takamasa Ishino[1] | Toshifumi Ninomiya[1] | Kiichiro Ninomiya[2] | Kota Tachibana[3] | Akiko Honobe-Tabuchi[4] | Yoshinori Muto[4] | Takashi Inozume[4,5] | Youki Ueda[1] | Kadoaki Ohashi[2] | Yoshinobu Maeda[2] | Joji Nagasaki[1] | Yosuke Togashi[1,6,7]

[1]Department of Tumor Microenvironment, Okayama University, Okayama, Japan | [2]Department of Hematology, Oncology and Respiratory Medicine, Okayama University, Okayama, Japan | [3]Department of Dermatology, Faculty of Medicine, Dentistry and Pharmaceutical Sciences, Okayama University, Okayama, Japan | [4]Department of Dermatology, University of Yamanashi, Yamanashi, Japan | [5]Department of Dermatology, Chiba University, Chiba, Japan | [6]Department of Allergy and Respiratory Medicine, Okayama University Hospital, Okayama, Japan | [7]Kindai University Faculty of Medicine, Osaka, Japan

Correspondence: Yosuke Togashi (ytogashi1584@gmail.com)

Received: 22 October 2024 | **Revised:** 12 February 2025 | **Accepted:** 17 February 2025

Funding: This research was supported by grants from the Japan Society for the Promotion of Science (JSPS) (JP20H03694 [Y. Togashi], JP21K20859 [T. Ishino], and JP22K15607 [K. Ninomiya]); Japan Agency for Medical Research and Development (AMED) (JP23ama221324h0001 [J. Nagasaki]); Japan Science and Technology Agency (JST) JPMJFR2049 (Y. Togashi); Canon Foundation (Y. Togashi); Daiichi Sankyo Foundation of Life Science (Y. Togashi); MSD Life Science Foundation (Y. Togashi); Japanese Respiratory Foundation (Y. Togashi); UBE Foundation (Y. Togashi); Ryobi Teien Memory Foundation (J. Nagasaki).

Keywords: antigenicity | cancer immunotherapy | CTLA-4 | PD-1 | regulatory T cell

ABSTRACT

Regulatory T (T_{reg}) cells have an immunosuppressive function, and programmed death-1 (PD-1)-expressing T_{reg} cells reportedly induce resistance to PD-1 blockade therapies through their reactivation. However, the effects of antigenicity on PD-1 expression in T_{reg} cells and the resistance to PD-1 blockade therapy remain unclear. Here, we show that T_{reg} cells gain high PD-1 expression through an antigen with high antigenicity. Additionally, tumors with high antigenicity for T_{reg} cells were resistant to PD-1 blockade in vivo due to PD-1^+ T_{reg}-cell infiltration. Because such PD-1^+ T_{reg} cells have high cytotoxic T lymphocyte antigen (CTLA)-4 expression, resistance could be overcome by combination with an anti-CTLA-4 monoclonal antibody (mAb). Patients who responded to combination therapy with anti-PD-1 and anti-CTLA-4 mAbs sequentially after primary resistance to PD-1 blockade monotherapy showed high T_{reg} cell infiltration. We propose that the high antigenicity of T_{reg} cells confers resistance to PD-1 blockade therapy via high PD-1 expression in T_{reg} cells, which can be overcome by combination therapy with an anti-CTLA-4 mAb.

1 | Introduction

Specific monoclonal antibodies (mAbs) against programmed death (PD)-1 or programmed death ligand-1 (PD-L1) have improved patient survival and have been approved for treating various cancer types [1, 2]. However, their efficacy remains insufficient, and various combination therapies, including combinations with anti-cytotoxic T lymphocyte antigen (CTLA)-4 mAbs, have been tried [3–9]. However, the combination therapies have increased immune-related adverse effects (irAEs)

Abbreviations: ADCC, antibody-dependent cellular cytotoxicity; CTLA-4, cytotoxic T lymphocyte antigen-4; eT_{reg} cell, effector regulatory T cell; FFPE, formalin fixed paraffin embedded; GITR, glucocorticoid-induced tumor necrosis factor receptor-related protein; ICI, immune checkpoint inhibitor; ICOS, inducible T-cell co-stimulator; irAEs, immune-related adverse event; mAb, monoclonal antibody; MHC-I, major histocompatibility complex class I; MHC-II, major histocompatibility complex class II; OVA, ovalbumin; PBMC, peripheral blood mononuclear cell; PD-1, programmed cell death-1; PD-L1, programmed cell death-1 ligand-1; TCR, T cell receptor; TIL, tumor-infiltrating lymphocytes; TME, tumor microenvironment; T_{reg} cell, regulatory T cell.

[10, 11]. Therefore, predictive biomarkers for combination therapies with anti-CTLA-4 mAbs are urgently required.

Regulatory T (T_{reg}) cells are highly immunosuppressive and contribute to the maintenance of self-tolerance and immune homeostasis [12, 13]. T_{reg} cells in the tumor microenvironment (TME) promote tumor progression [14, 15]. Previous studies have reported that PD-1$^+$ T_{reg} cells in the TME could be associated with resistance to PD-1 blockade therapy through their reactivation [16–18]. Antigenicity plays an important role in PD-1 expression in T cells [16, 19], whereas the effects of antigenicity on PD-1 expression in T_{reg} cells and resistance to PD-1 blockade therapy remain unclear. Furthermore, CTLA-4 is a crucial molecule for T_{reg}-cell-mediated immune suppression, and anti-CTLA-4 mAbs can inhibit T_{reg} cells [12, 13]. However, the effects of anti-CTLA-4 mAbs on PD-1$^+$ T_{reg} cells in the TME remain unclear.

In this study, we investigated the role of antigenicity for T_{reg} cells in PD-1 expression in T_{reg} cells and found that high antigenicity of T_{reg} cells induced high PD-1 expression in T_{reg} cells. Mouse tumors with high antigenicity for T_{reg} cells were resistant to PD-1 blockade by PD-1$^+$ T_{reg} cells. Additionally, resistant tumors responded to a combination of anti-PD-1 and anti-CTLA-4 mAbs. We propose that the high antigenicity for T_{reg} cells confers resistance to PD-1 blockade therapy via high PD-1 expression in T_{reg} cells, which can be overcome by combination therapy with anti-CTLA-4 mAbs.

2 | Materials and Methods

2.1 | T Cell Receptor Stimulation Assays

To evaluate PD-1 expression in T cells, peripheral blood mononuclear cells (PBMCs) from three healthy volunteers or splenocytes from female C57BL/6J mice (Japan SLC, Shizuoka, JPN) were cultured with indicated concentrations of anti-CD3 mAb (human, clone OKT3, Thermo Fisher Scientific, Waltham, MA; mouse, clone 145-2C11, BioLegend, San Diego, CA), 10 μg/mL anti-CD28 mAb (human, clone CD28.2, Thermo Fisher Scientific; mouse, clone 37.51, BioLegend), and 30 IU/mL IL-2 (PeproTech, Cranbury, NJ) for 48 h and then subjected to flow cytometry. The protocol was approved by the appropriate institutional review board and ethics committee of Okayama University Hospital.

2.2 | Suppression Assays

PD-1$^-$CD8$^+$ T cells and PD-1$^-$ or PD-1$^+$CD25$^+$CD4$^+$ T cells (T_{reg} cells) were sorted from mouse splenocytes using a FACSAria instrument (BD Biosciences, Franklin Lakes, NJ). A total of 2×10^4 CTV (Thermo Fisher Scientific)-labeled responder CD8$^+$ T cells (T_{resp} cells) were cocultured with or without unlabeled 2×10^4 T_{reg} cells in the presence of gamma-irradiated antigen-presenting cells (APCs) (CD4$^+$ and CD8$^+$ T-cell depleted splenocytes) and 1 μg/mL anti-CD3 mAb. In some wells, 20 μg/mL anti-mouse PD-1 (clone RMP1-14, BioLegend) was added. The dilution of CTV-labeled cells was assessed 3 days later with flow cytometry.

2.3 | Prediction of Binding Affinity of Ovalbumin Peptides

We predicted the binding affinities to mouse MHC class II (MHC-II), I-A^b using NetMHCIIpan 4.0 [20, 21]. The total ovalbumin (OVA) peptide reportedly includes peptides presented by MHC class I (MHC-I) (OVA-I, SIINFEKL [257–264]) and MHC-II (OVA-II, ISQAVHAAHAEINEAGR [323–339]) (Figure S1A) [22, 23]. We used ISQAVHAAHAEINEAGR, ISQAVHAAFAEINEAGR, and ISQAVHAARAEINEAGR as the OVA-II, OVA-II (F), and OVA-II (R) peptides, respectively.

2.4 | Peptide Pulse Assays

The following OVA peptides were obtained from Synpeptide (Shanghai, China): OVA-I, OVA-II, OVA-II (F), and OVA-II (R). CD25$^+$CD4$^+$ T_{reg} cells were purified from female C57BL/6J or B6.Cg-Tg(TcraTcrb)425Cbn/J mice (*OT-II*; IMSR_JAX:004194, Jackson Laboratories) splenocytes using a FACSAria instrument. These cells were stimulated with gamma-irradiated APCs pulsed with the various peptides at a 10 μM concentration. APCs were added to round-bottom 96-well plates containing purified T_{reg} cells. After 48 h, presensitized T_{reg} cells were analyzed using flow cytometry.

2.5 | Cell Lines

B16F10 and LL/2 cell lines were purchased from ATCC (Manassas, VA). The B16F10 and LL/2 cell lines were maintained in RPMI 1640 medium supplemented with 10% FBS (Thermo Fisher Science). All cell lines were used after confirming mycoplasma negativity using the PCR Mycoplasma Detection Kit (Takara Bio, Shiga, JPN).

2.6 | Constructs and Viral Production

The following constructs were gifts: pcDNA3-*TfR-OVA*, from Sandra Diebold and Martin Zenke (Addgene plasmid #64600; http://n2t.net/addgene:64600) [24], and pBABE-puro, from Hartmut Land and Jay Morgenstern & Bob Weinberg (Addgene plasmid #1764; http://n2t.net/addgene:1764) [25]. *TfR-OVA* cDNA was cloned into the pBABE-puro vector using In-Fusion Snap Assembly Master Mix (Takara Bio). The OVA-I and OVA-II epitopes were deleted from the pBABE-puro-*TfR-OVA* vector using a KOD-Plus mutagenesis kit (TOYOBO, Osaka, JPN) to obtain pBABE-puro-*TfR-OVA-II* and pBABE-puro-*TfR-OVA-I*, respectively (Figure S1A). Additionally, an H331F mutation in *OVA* was introduced into the pBABE-puro-*TfR-OVA-II* vector using the KOD-Plus mutagenesis kit and designated pBABE-puro-*TfR-OVA-II* (F) (Figure S1B).

pBABE-puro-*TfR-OVA-I*, pBABE-puro-*TfR-OVA-II*, or pBABE-puro-*TfR-OVA-II* (F) vector was transfected with pVSV-G vector (Takara Bio) into packaging cells using Lipofectamine 3000 Reagent (Thermo Fisher Scientific). After 48 h, the supernatant was concentrated and transfected into the cells. B16F10 cells transfected with *TfR-OVA*, *TfR-OVA-I*, *TfR-OVA-II*, or *TfR-OVA-II* (F) were designated B16F10/OVA, B16F10/OVA-I,

B16F10/OVA-II, or B16F10/OVA-II (F), respectively. The LL/2 cell line transfected with *TfR-OVA* was designated LL2/OVA.

2.7 | Quantitative Real-Time Reverse Transcription PCR

Total RNA was reverse-transcribed to cDNA using PrimeScript RT Master Mix (Takara Bio), and real-time PCR was performed using TB Green Premix Ex Taq II (Takara Bio). *Gapdh* was used as an internal control. For each sample, ΔC_t for *OVA* versus *Gapdh* was calculated as $\Delta C_t = C_t$ (*OVA*)—C_t (*Gapdh*). In vitro experiments were performed in triplicates. The used primers are summarized in Table S1.

2.8 | Coculture Assays

Purified WT or OT-II $CD25^+CD4^+$ T_{reg} cells or bulk splenocytes from female C57BL/6J mice or OT-II mice were cocultured with OVA-overexpressing cancer cells for 48 h. Afterward, PD-1 expression in T_{reg} cells was analyzed with flow cytometry.

2.9 | Mouse Study

C57BL/6J-Prkdc<scid>/Rbrc mice (B6 SCID; RBRC01346) were provided by RIKEN BRC through the National BioResource Project of the MEXT/AMED, Japan. 5×10^5 (B16F10) or 1×10^6 (LL/2) cells were injected subcutaneously on day 0, and the tumor volume was monitored twice a week. 5×10^6 $CD8^+$ T cells sorted from wild-type C57BL/6J splenocytes and/or 5×10^5 $CD25^+CD4^+$ T_{reg} cells sorted from wild-type C57BL/6J or *OT-II* splenocytes using a FACSAria instrument were injected intravenously on day 4. Anti-PD-1 (200 μg/mouse, clone RMP1-14, BioLegend), anti-CTLA-4 IgG2a (200 μg/mouse, clone 9D9, Absolute Antibody, Wilton, UK), and/or control mAbs (clone RTK2758, BioLegend) were administered intraperitoneally three times every 3 days from day 5 onwards. Additionally, a combination of anti-PD-1 and CTLA-4 IgG2a mAbs was administered intraperitoneally three times every 3 days from day 14 after anti-PD-1 mAb alone. Tumors were harvested on day 8 or 12 for tumor-infiltrating lymphocytes (TIL) analysis.

In vivo experiments were performed at least twice. All animals were bred and housed under specific pathogen-free conditions at Okayama University. The animal experiments were approved by the Animal Committee for Animal Experimentation of Okayama University. All experiments adhered to the U.S. Public Health Service Policy on Human Care and Use of Laboratory Animals.

2.10 | Flow Cytometry

Flow cytometry assays were performed as previously described [16, 17]. Briefly, the cells were washed with phosphate-buffered saline containing 2% FBS and stained with surface antibodies. Intracellular staining was performed with specific antibodies and a FOXP3/Transcription Factor Staining Buffer Set (Thermo Fisher Scientific). When PD-L1, CD80, CD86, and MHC-II expression in cancer cells were evaluated in vitro, cancer cells were treated with or without IFN-γ (10 ng/mL, PeproTech) for 48 h. The samples were assessed using a BD FACSFortessa instrument (BD Biosciences) and FlowJo software (BD Biosciences). The staining antibodies are summarized in Table S2.

2.11 | Patients and Immunohistochemistry

Two patients with advanced melanoma responded to the combination therapy with nivolumab and ipilimumab sequentially after primary resistance to anti-PD-1 mAb monotherapy between 2015 and 2020 at Okayama University Hospital or Yamanashi University Hospital, and their formalin-fixed paraffin-embedded (FFPE) samples before the initiation of anti-PD-1 mAb monotherapy were obtained. Additionally, FFPE samples were obtained before the initiation of anti-PD-1 mAb monotherapy from four non-responders with advanced melanoma to the combination therapy sequentially after primary resistance to anti-PD-1 mAb monotherapy between 2019 and 2020 at Okayama University Hospital. Primary resistance was defined as disease progression at the first evaluation or < 6 months of stable disease without any tumor shrinkage. Patients' clinical information is summarized in Table S3. The protocols were approved by the appropriate institutional review boards and ethics committees of Okayama University Hospital and Yamanashi University Hospital.

FFPE sections (3 μm) were deparaffinized, rehydrated, and subjected to antigen retrieval. After permeabilization, individual slides were incubated with an anti-Foxp3 mAb (clone 236A/E7, Abcam, Cambridge, UK) overnight at 4°C. After inhibiting endogenous peroxidase activity, slides were incubated for 30 min with SingleStain Boost Immunohistochemistry (IHC) Detection Reagent (Cell Signaling Technology, Danvers, MA). They were then treated with a DAB substrate kit (Cell Signaling Technology). Nuclear counterstaining was performed using Giemsa staining solution to differentiate between melanin pigment and DAB color development.

2.12 | Statistical Analyses

GraphPad Prism 8 (GraphPad Software, San Diego, CA) was used for statistical analyses. The relationship between continuous variables between or among groups was compared using a *t*-test or one-way ANOVA, respectively. The relationship between tumor volume curves was compared using two-way ANOVA. For multiple testing, a Bonferroni correction was employed. Statistical significance was set at $p < 0.05$. All statistical details are provided in the figure legends.

3 | Results

3.1 | Stronger TCR Stimulation Induces Higher PD-1 Expression in T_{reg} Cells

First, we treated PBMCs with anti-CD3 and anti-CD28 mAbs. Similar to previous reports, PD-1 expression in $CD8^+$ T cells increased in an anti-CD3 mAb concentration-dependent

manner (Figure S2A). Next, we investigated PD-1 expression in T_{reg} cells. Because naïve human $CD4^+$ T cells transiently upregulate Foxp3 expression upon T cell receptor (TCR) stimulation, $Foxp3^+$ T cells in humans comprise suppressive T_{reg} and non-suppressive conventional T cells [26]. Therefore, we fractionated $CD4^+Foxp3^+$ T cells into three subsets based on their expression levels of the naïve T-cell markers CD45RA and Foxp3: Fr I, naïve T_{reg} cells ($CD45RA^+Foxp3^{low}CD4^+$) with weak immunosuppressive function; Fr II, effector Treg (eT_{reg}) cells ($CD45RA^-Foxp3^{high}CD4^+$) with strong immunosuppressive function; and Fr III, non-Treg cells ($CD45RA^-Foxp3^{low}CD4^+$) with no immunosuppressive function (Figure 1A) [13, 27]. PD-1 expression in eT_{reg} cells also increased in a concentration-dependent manner (Figure 1B). Additionally, the expression of T_{reg}-cell activation-related molecules, such as CTLA-4, inducible T-cell co-stimulator (ICOS), and glucocorticoid-induced tumor necrosis factor receptor-related protein (GITR), increased (Figure 1C–E). Accordingly, PD-1^+ eT_{reg} cells had significantly higher expression levels of these molecules than PD-1^- eT_{reg} cells (Figure 1F). Similar findings were observed in the mouse splenocytes (Figure 2A–E and Figure S2B). These results indicate that stronger TCR stimulation induces higher PD-1 expression and activation in T_{reg} as well as $CD8^+$ T cells.

3.2 | Activated Suppressive Function of PD-1^+ T_{reg} Cells Is Further Amplified by PD-1 Blockade

We next performed suppression assays using PD-1^- or PD-$1^+CD25^+CD4^+$ T_{reg} cells. The proliferation of T_{resp} cells was examined with CTV-labeled PD-1^-CD8^+ T cells cocultured with or without T_{reg} cells. When T_{resp} cells were cocultured with PD-1^- T_{reg} cells, the proliferation of T_{resp} cells was comparable by PD-1 blockade (Figure 2F). In contrast, PD-1^+ T_{reg} cells showed a little activated immunosuppressive function compared with PD-1^- ones, and the proliferation of T_{resp} cells was much more strongly inhibited by PD-1 blockade, indicating further amplification of activated PD-1^+ T_{reg} cells (Figure 2F).

3.3 | Antigenicity for T_{reg} Cells Plays Important Roles in PD-1 Expression and Activation in T_{reg} Cells Both In Vitro and In Vivo

Since strong TCR stimulation indicates high antigenicity, we used an OVA peptide as an antigen with high antigenicity for T_{reg} cells. The total OVA sequence reportedly includes both OVA-I and OVA-II epitopes, which can induce $CD8^+$ and $CD4^+$ T-cell activation, respectively (Figure S1A) [22, 23]. As expected, when T_{reg} cells were stimulated with the OVA-II peptide in vitro, the cells from *OT-II* mice (OT-II T_{reg} cells) showed significantly higher PD-1 expression than those from wild-type mice (WT T_{reg} cells) (Figure S3A). Similar trends were observed for CTLA-4, ICOS, and GITR expression (Figure S3B–D). Additionally, PD-1^+ T_{reg} cells stimulated by the OVA-II peptide had significantly higher expression levels of these molecules than PD-1^- T_{reg} cells (Figure S3E).

Because OVA-specific T_{reg} cells in wild-type mice are extremely scarce, we next used OVA peptides with various antigenicities for OVA-specific OT-II T_{reg} cells. The OVA-II (F) and (R) peptides from H331F- and H331R-mutated *OVA*, respectively, reportedly induce weak TCR signaling in *OT-II* TCR compared with the wild-type OVA-II peptide [23, 28, 29]. Additionally, we predicted the binding affinities to A-I^b of these OVA peptides using NetMHCIIpan 4.0 [20, 21]. The predicted binding affinities of the OVA-II (F) and (R) peptides were slightly lower than those of the OVA-II peptide, whereas that of the OVA-I peptide was very low (Figure S1C). Then, we used OVA-I, OVA-II (F), OVA-II (R), and OVA-II peptides with various antigenicities to stimulate OT-II T_{reg} cells. OVA-I, with little antigenicity for $CD4^+$ T cells, did not induce PD-1 expression in OT-II T_{reg} cells; however, OVA-II (F) and (R), with antigenicity for $CD4^+$ T cells, induced PD-1 expression in OT-II T_{reg} cells (Figure 3A). Additionally, OVA-II, which had the highest antigenicity, further induced PD-1 expression in OT-II T_{reg} cells (Figure 3A). Similar trends were observed for CTLA-4, ICOS, and GITR expression in OT-II T_{reg} cells (Figure 3B–D).

To validate these findings in vivo, we created *OVA*-overexpressing B16F10 and LL/2 cell lines (B16F10/OVA, B16F10/OVA-I, B16F10/OVA-II [F], B16F10/OVA-II, and LL2/OVA) and adjusted OVA expression equally (Figure S1A,B,D). PD-L1 expression in B16F10/OVA and LL2/OVA cells increased following IFN-γ treatment, while CD80, CD86, and MHC-II were scarcely expressed (Figure S4A). Accordingly, PD-1 expression in WT or OT-II T_{reg} cells cocultured with OVA-overexpressing cancer cells using purified T_{reg} cells showed little increase in vitro, possibly due to the lack of MHC-II expression (Figure S4B). In contrast, PD-1 expression in gated T_{reg} cells cocultured with OVA-overexpressing cancer cells using bulk splenocytes increased in vitro, with PD-1 expression being higher in OT-II T_{reg} cells than in WT T_{reg} cells (Figure S4B). These findings suggest that the cancer cells themselves do not present the OVA-II peptide and that APCs are required for T_{reg} cells to recognize the peptide. These tumors were inoculated into B6 SCID mice, and OT-II T_{reg} cells were transferred; then we analyzed PD-1 expression in tumor-infiltrating OT-II T_{reg} cells (Figure 4A). These cancer cells had PD-L1 but had scarce CD80, CD86, and MHC-II expression in vivo (Figure S4C). In contrast, APCs such as dendritic cells in TILs had these molecules (Figure S4C). PD-1 expression in T_{reg} cells in B16F10/OVA-I tumors was comparable to that in parental tumors (Figure 4B). In contrast, PD-1 expression in T_{reg} cells in B16F10/OVA-II (F) tumors was higher than that in parental tumors. Furthermore, T_{reg} cells in B16F10/OVA-II tumors showed the highest PD-1 expression (Figure 4B). Similar trends were observed in CTLA-4, ICOS, and GITR expression (Figure 4C–E). Taken together, the high antigenicity of T_{reg} cells induces high PD-1 expression and activation in T_{reg} cells both in vitro and in vivo.

3.4 | High Antigenicity for T_{reg} Cells Impairs Antitumor Immunity Including PD-1 Blockade-Mediated One

We treated *OVA*-overexpressing tumors (B16F10 or LL/2) in B6 SCID mice with T cell transfer and/or ICIs to evaluate the relationship between the antigenicity of T_{reg} cells and antitumor immunity (Figure 5A). When $CD8^+$ T cells from wild-type mice (WT $CD8^+$ T cells) were transferred, B16F10/OVA tumors grew

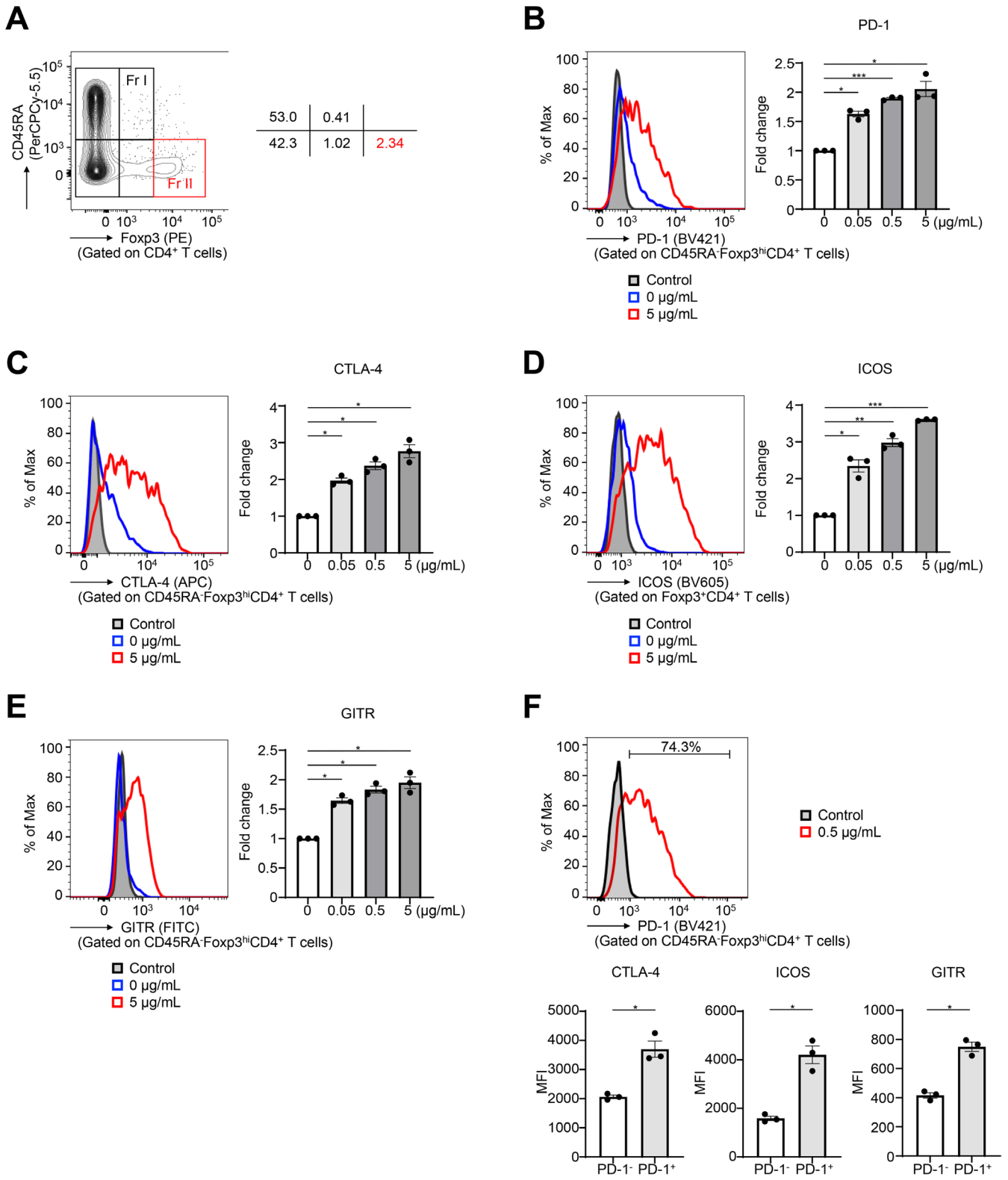

FIGURE 1 | Relationship between TCR stimulation and PD-1 expression in human eT_{reg} cells. (A) Gating strategy for eT_{reg} cells. To analyze eT_{reg} cells, we used CD45RA and Foxp3, and defined $CD45RA^{-}Foxp3^{high}CD4^{+}$ T cells as eT_{reg} cells. (B–E) PD-1 (B), CTLA-4 (C), ICOS (D), and GITR (E) expression in eT_{reg} cells. Peripheral blood mononuclear cells (PBMCs) were cultured with anti-CD3 and anti-CD28 mAbs, and IL-2 for 48 h and subjected to flow cytometry. Fold changes were calculated by normalizing the mean fluorescence intensity (MFI) of the no-antibody group (0 μg/mL) to 1. Representative flow cytometry staining (left) and summaries (right) are shown ($n = 3$). (F) CTLA-4, ICOS, and GITR in eT_{reg} cells according to PD-1 expression in the condition with 0.5 μg/mL anti-CD3 mAb. In vitro experiments were performed as described in (B–E). Gating strategy for PD-1 expression (top) and summaries (bottom/left, CTLA-4; bottom/middle, ICOS; and bottom/right, GITR) are shown ($n = 3$). $^{*}p < 0.05$; $^{**}p < 0.01$; $^{***}p < 0.001$; bars, mean; error bars, SEM.

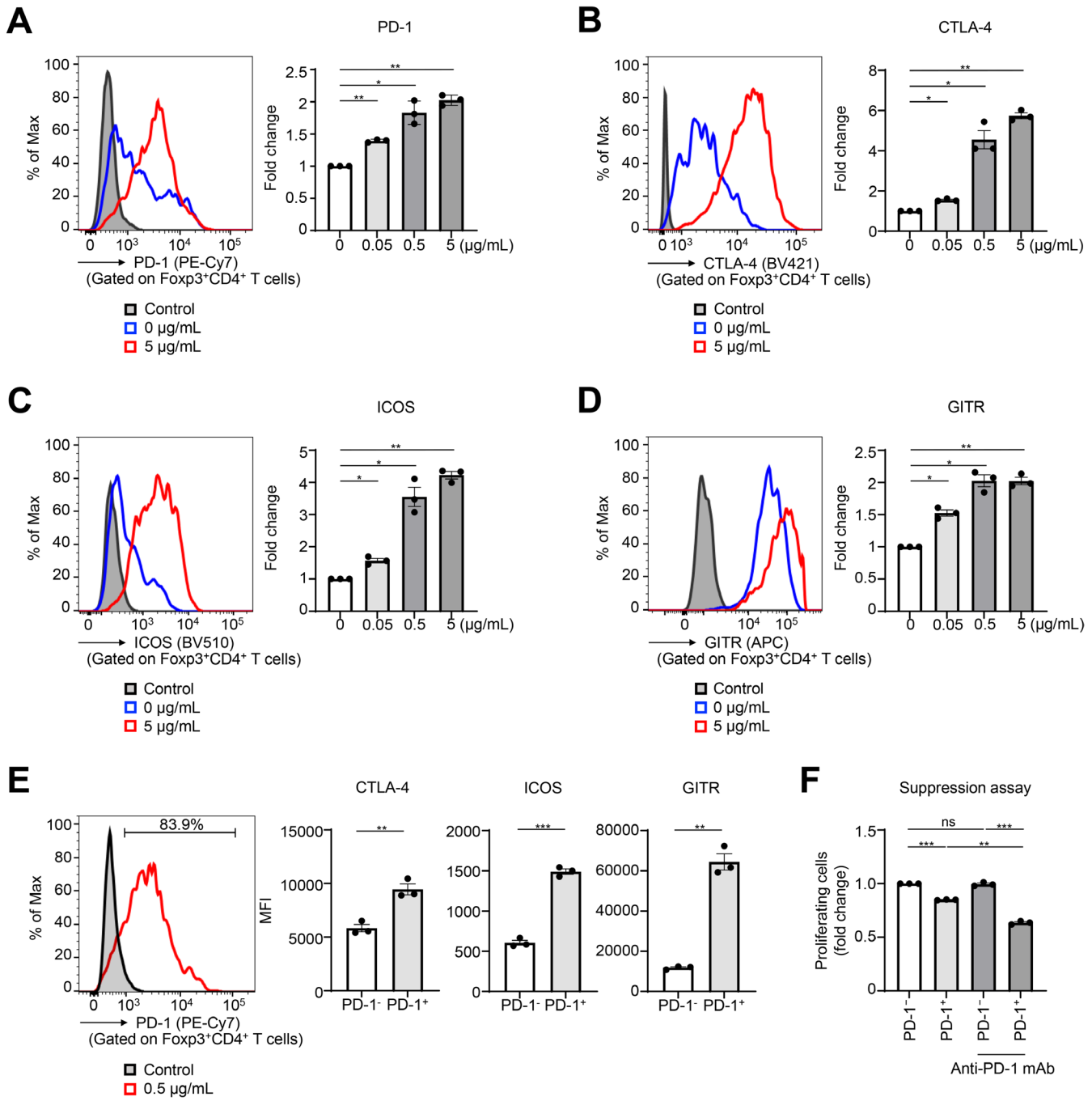

FIGURE 2 | Relationship between TCR stimulation and PD-1 expression in mouse T_{reg} cells, and their suppressive function according to PD-1 expression. (A–D) PD-1 (A), CTLA-4 (B), ICOS (C), and GITR (D) expression in T_{reg} cells. Splenocytes from C57BL/6J mice were cultured with anti-CD3 and anti-CD28 mAbs, and IL-2 for 48 h and subjected to flow cytometry. Fold changes were calculated by normalizing the mean fluorescence intensity (MFI) of the no-antibody group (0 μg/mL) to 1. Representative flow cytometry staining (left) and summaries (right) are shown ($n = 3$). (E) CTLA-4, ICOS, and GITR in T_{reg} cells according to PD-1 expression in the condition with 0.5 μg/mL anti-CD3 mAb. In vitro experiments were performed as described in (A–D). Gating strategy for PD-1 expression (leftmost) and summaries (second from the left, CTLA-4; second from the right, ICOS; and rightmost, GITR) are shown ($n = 3$). (F) Suppression assay of T_{reg} cells. CTV-labeled responder $CD8^+$ T cells (T_{resp} cells) from mouse splenocytes were cocultured with or without unlabeled sorted PD-1^- or PD-1^+ T_{reg} cells. Anti-PD-1 mAb was added to some wells. The proliferation of T_{resp} cells was assessed 3 days later by dilution of CTV-labeled cells using flow cytometry. The fold change in CTV dilution of T_{resp} cells was calculated. Summary is shown ($n = 3$). $^*p < 0.05$; $^{**}p < 0.01$; $^{***}p < 0.001$; bars, mean; error bars, SEM.

slowly compared to those in the control (Figure S5A). In addition, PD-1 blockade exhibited dramatic efficacy. In contrast, additional WT T_{reg}-cell transfer induced rapid growth compared to $CD8^+$ T cell transfer alone. Under this condition, the tumors were slightly resistant to PD-1 blockade (Figure S5A).

Next, we transferred OT-II T_{reg} cells, in addition to WT $CD8^+$ T cells (Figure 5A). Because OVA-II has high antigenicity for OT-II T_{reg} cells, tumor-infiltrating OT-II T_{reg} cells exhibited significantly higher PD-1, CTLA-4, ICOS, and GITR expression than WT T_{reg} cells, indicating that tumor-infiltrating

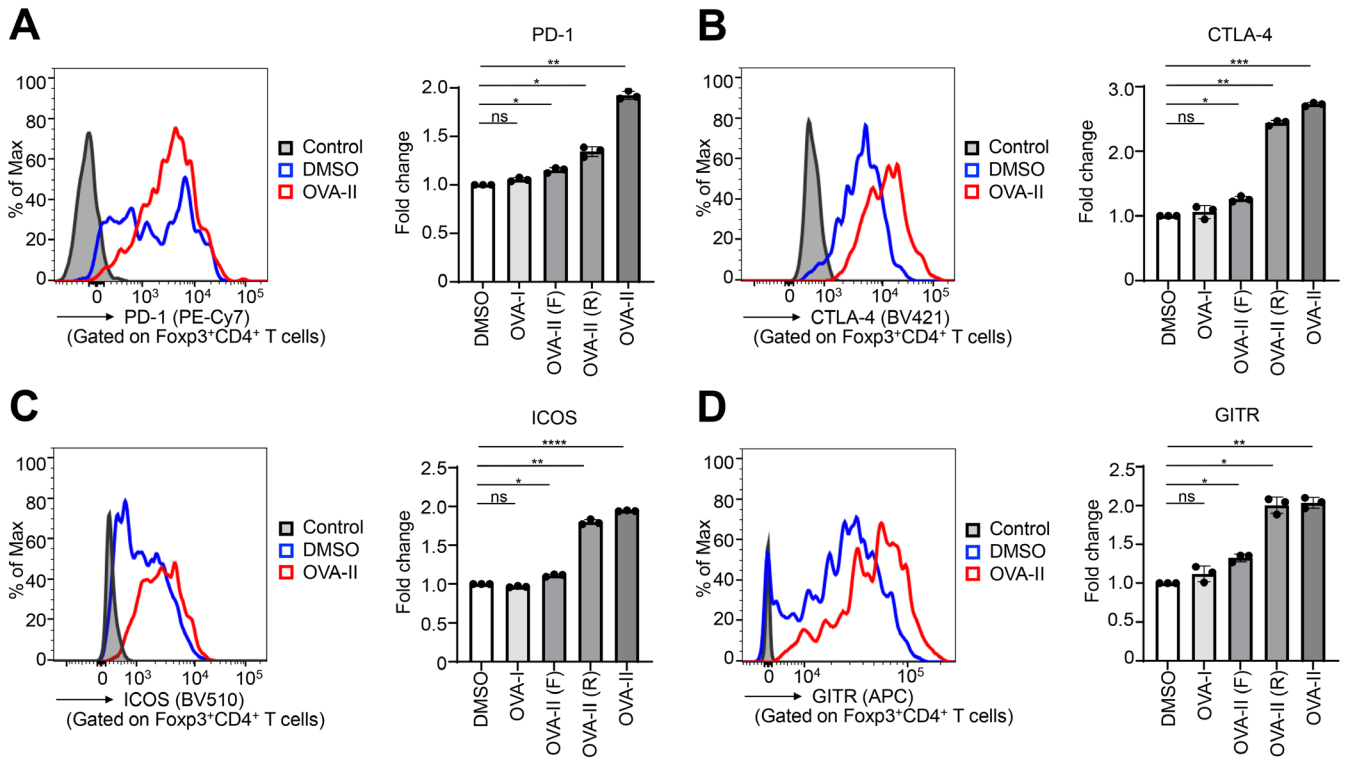

FIGURE 3 | Relationship between antigenicity and PD-1 expression in T_{reg} cells in vitro. PD-1 (A), CTLA-4 (B), ICOS (C), and GITR (D) expression in OT-II T_{reg} cells. $CD25^+CD4^+$ T_{reg} cells were purified from *OT-II* splenocytes and stimulated with gamma-irradiated antigen-presenting cells pulsed with various peptides (OVA-I, SIINFEKL; OVA-II, ISQAVHAAHAEINEAGR; OVA-II (F), ISQAVHAAFAEINEAGR; and OVA-II (R), ISQAVHAARAEINEAGR). After 48 h, presensitized T_{reg} cells were analyzed with flow cytometry. Fold changes were calculated by normalizing the mean fluorescence intensity of DMSO to 1. Representative flow cytometry staining (left) and summaries (right) are shown ($n = 3$). $^*p < 0.05$; $^{**}p < 0.01$; $^{***}p < 0.001$; $^{****}p < 0.0001$; ns, not significant; bars, mean; error bars, SEM.

OT-II T_{reg} cells were activated in *OVA*-overexpressing tumors (Figure 5B–E). Similar to in vitro data, $PD\text{-}1^+$ OT-II T_{reg} cells had significantly higher expression levels of CTLA-4, ICOS, and GITR than $PD\text{-}1^-$ OT-II T_{reg} cells in B16F10/OVA-II tumors (Figure 5F). The transfer of OT-II T_{reg} cells induced rapid growth compared to WT T_{reg}-cell transfer (Figure 6A and Figure S5B). In addition, this model (WT $CD8^+$ T and OT-II T_{reg} cells) was resistant to PD-1 blockade compared to the WT $CD8^+$ T and WT T_{reg} cell transfer model (Figure 6A and Figure S5B). Because previous reports have shown that PD-1 blockade activates $PD\text{-}1^+$ T_{reg}-cell mediated suppressive functions [16–18], we analyzed and compared TILs treated with PD-1 blockade (Figure 5A). The results showed that PD-1 blockade increased T_{reg}-cell activation-related molecule expression in tumor-infiltrating OT-II T_{reg} cells and the $T_{reg}/CD8^+$ T cell ratio, which is consistent with previous studies (Figure 6B–G) [16–18]. As $PD\text{-}1^+$ T_{reg} cells showed high CTLA-4 expression, as shown in Figure 5F, we added an anti-CTLA-4 IgG2a mAb with antibody-dependent cellular cytotoxic activity (ADCC) to this model. Notably, an anti-CTLA-4 IgG2a mAb reversed the resistance and reduced the $T_{reg}/CD8^+$ T cell ratio in TILs, whereas the anti-CTLA-4 IgG2a mAb alone exhibited efficacy comparable to that of PD-1 blockade alone (Figure 6A,G and Figure S5B–D). Additionally, the combination therapy following anti-PD-1 mAb alone also reversed the resistance (Figure S5C,D). Overall, these results suggest that the high antigenicity for T_{reg} cells impairs antitumor immunity and confers resistance to PD-1 blockade via $PD\text{-}1^+$ T_{reg} cells. Anti-CTLA-4 mAbs can target such T_{reg} cells and overcome this resistance.

3.5 | Patients Who Are Resistant to Anti-PD-1 mAb Monotherapy due to T_{reg} Cell Infiltration Can Respond to Combination Therapy With Anti-PD-1 and Anti-CTLA-4 mAbs

Finally, we analyzed clinical samples from patients with advanced melanoma who received combination therapy with anti-PD-1 and anti-CTLA-4 mAbs, sequentially after primary resistance to anti-PD-1 mAb monotherapy (Table S3). Two patients (cases 1 and 2) who responded to combination therapy sequentially after resistance to monotherapy showed high T_{reg} cell infiltration (Figure 7A,B,D). In contrast, four patients (cases 3–6) who failed to respond showed little T_{reg} cell infiltration (Figure 7C,E). These results support our experimental findings, suggesting that $PD\text{-}1^+$ T_{reg} cell infiltration can be used as a predictive biomarker for combination therapy with anti-PD-1 and anti-CTLA-4 mAbs.

4 | Discussion

PD-1 generally suppresses effector functions in effector T cells, mainly by inhibiting TCR signaling pathways [30]. In addition to effector T cells, PD-1 plays a suppressive role in T_{reg} cells,

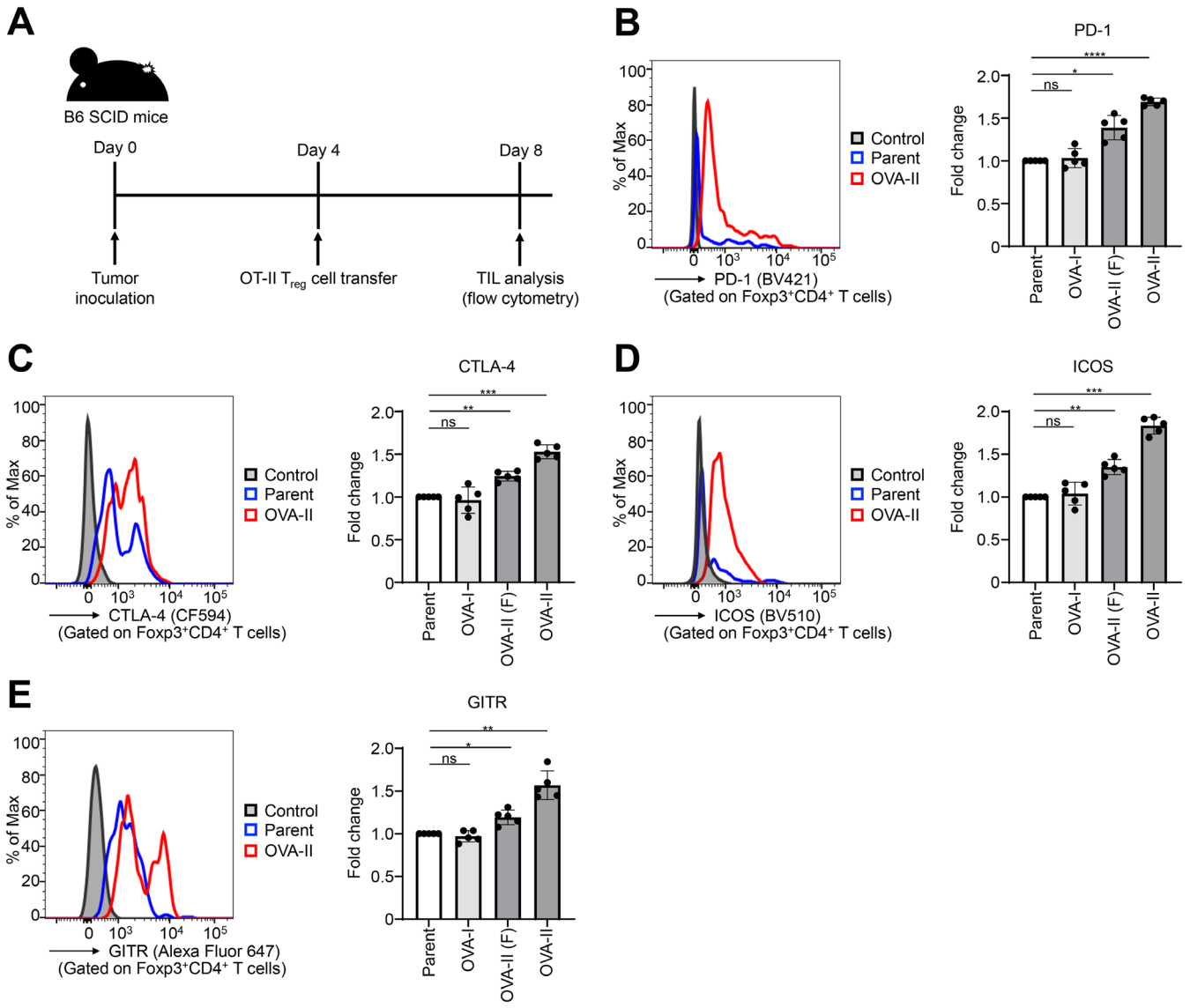

FIGURE 4 | Relationship between antigenicity and PD-1 expression in tumor-infiltrating T_{reg} cells in vivo. (A) Experimental scheme. 5×10^5 parental B16F10, B16F10/OVA-I, B16F10/OVA-II (F), or B16F10/OVA-II cells were injected subcutaneously into B6 SCID mice on day 0. Subsequently, 5×10^5 OT-II T_{reg} cells were injected intravenously on day 4. Tumors were harvested on day 8 for tumor-infiltrating lymphocyte (TIL) analysis with flow cytometry. (B–E) PD-1 (B), CTLA-4 (C), ICOS (D), and GITR (E) expression in tumor-infiltrating OT-II T_{reg} cells. Representative flow cytometry staining (left) and summaries (right) are shown ($n = 5$). *$p < 0.05$; **$p < 0.01$; ***$p < 0.001$; ****$p < 0.0001$; ns, not significant; bars, mean; error bars, SEM.

which can be activated by PD-1 blockade [16–18]. PD-1 is highly expressed in tumor-infiltrating T_{reg} cells, and PD-1 blockade activates suppressive functions in PD-1$^+$ T_{reg} cells, leading to resistance to PD-1 blockade therapies [16–18]. However, the detailed mechanism of PD-1 expression in tumor-infiltrating T_{reg} cells remains unclear. We previously showed that the glycolytic TME promotes PD-1 expression in T_{reg} cells [31]. Here, we additionally demonstrated that the antigenicity of T_{reg} cells was important for PD-1 expression, leading to resistance to PD-1 blockade therapies.

During thymic development, thymocytes, which strongly bind self-peptides presented by medullary thymic epithelial cells, undergo apoptosis, a process called negative selection [32]. However, some CD4$^+$CD8$^-$ thymocytes that receive relatively strong TCR stimulation from self-peptides subsequently differentiate into T_{reg} cells [33–36]. A recent study showed that the development of T_{reg} cells occurs in response to strong but disrupted stimulation by self-antigens [37]. Therefore, the TCR repertoire of T_{reg} cells tends to be enriched for self-specificity. In the present study, T_{reg} cell antigens in tumors promoted PD-1 expression in tumor-infiltrating T_{reg} cells and conferred resistance to PD-1 blockade therapies. Therefore, the T_{reg} cell antigens, as well as PD-1$^+$ T_{reg} cell infiltration, can be used as resistance biomarkers. However, evaluating T_{reg} cell antigens accurately can be difficult because they could have self-specificities [33–36]. In contrast, several other studies have shown that T_{reg} cells in tumors recognize somatic mutation-derived neoantigens [38, 39]. Therefore, further studies are warranted to elucidate the role of T_{reg} cell antigens in tumors.

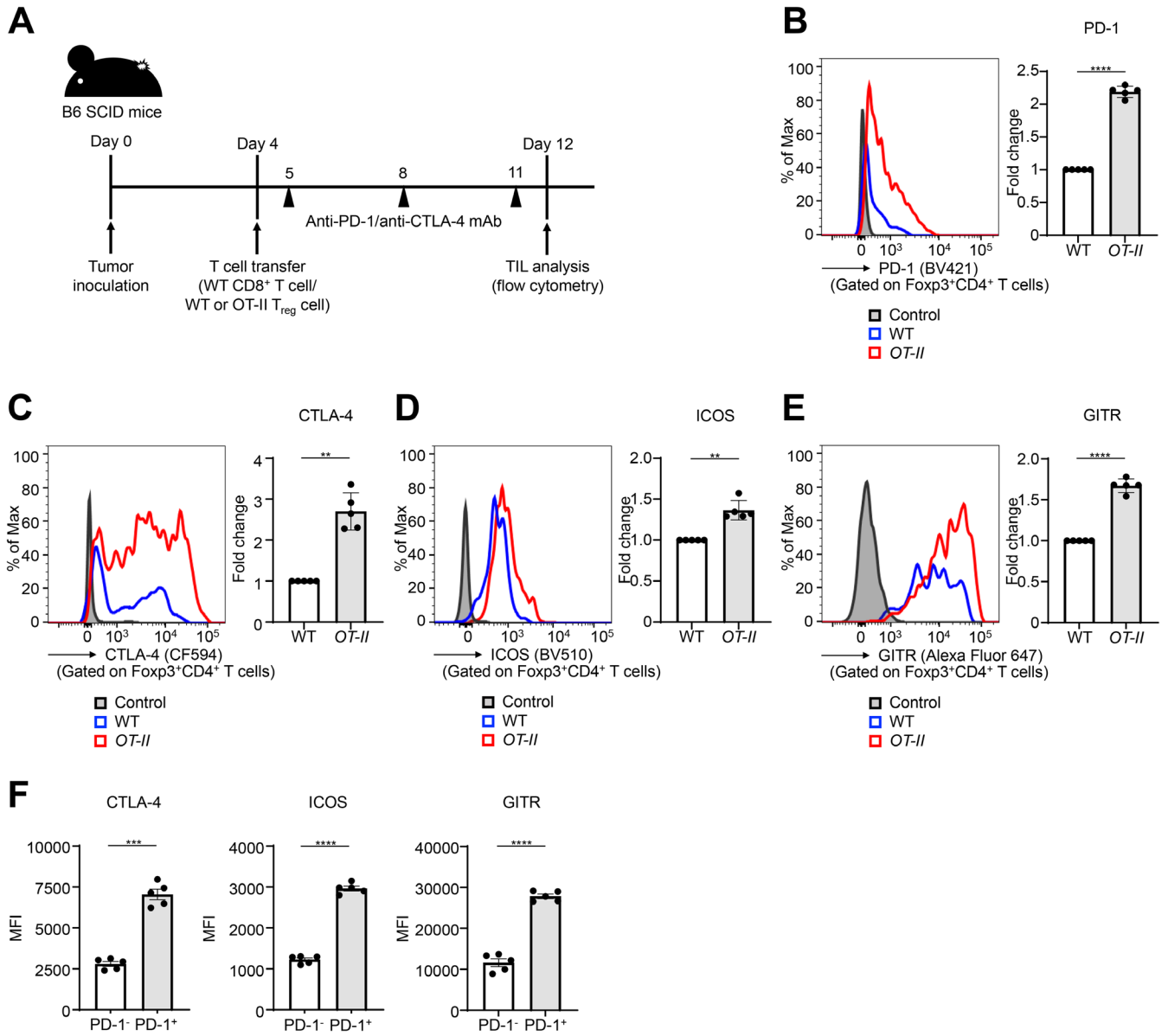

FIGURE 5 | Analyses of tumor-infiltrating WT and OT-II T_{reg} cells in adoptive T-cell transfer models. (A) Experimental scheme. 5×10^5 B16F10/OVA or 1×10^6 LL2/OVA cells were injected subcutaneously into B6 SCID mice on day 0. Subsequently, 5×10^6 WT $CD8^+$ T cells and/or 5×10^5 WT or OT-II T_{reg} cells were injected intravenously on day 4. Anti-PD-1, anti-CTLA-4 IgG2a, or control mAbs were administered intraperitoneally from day 5 onwards three times every 3 days. B16F10 tumors were harvested on day 12 for TIL analysis with flow cytometry. (B–E) PD-1 (B), CTLA-4 (C), ICOS (D), and GITR (E) expression in tumor-infiltrating WT and OT-II T_{reg} cells. Representative flow cytometry staining (left) and summaries (right) are shown ($n=5$). (F) CTLA-4, ICOS, and GITR in tumor-infiltrating OT-II T_{reg} cells according to PD-1 expression. Summaries (left, CTLA-4; middle, ICOS; and right, GITR) are shown ($n=5$). MFI, mean fluorescence intensity; $^{**}p<0.01$; $^{***}p<0.001$; $^{****}p<0.0001$; bars or lines, mean; error bars, SEM.

Anti-CTLA-4 mAbs have been used for the treatment of various cancer types in combination with PD-1 blockade therapies, and some patients achieved durable responses like the case 1 [3–9]. However, in a recent Japanese clinical trial, severe irAEs were observed, forcing the trial to stop [10, 11]. Therefore, predictive biomarkers for combination therapy with anti-CTLA-4 mAbs are required. In this study, PD-1^+ T_{reg} cells exhibited high CTLA-4 expression. Accordingly, an anti-CTLA-4 mAb with ADCC activity reduced tumor-infiltrating T_{reg} cells, which is consistent with previous reports [40–44], and overcame the resistance to PD-1 blockade due to PD-1^+ T_{reg} cells. Although our study had a small sample size, this is the first study to show that patients who responded to combination therapy with anti-PD-1 and anti-CTLA-4 mAbs sequentially after primary resistance to PD-1 blockade monotherapy had high T_{reg} cell infiltration. Consistently, the combination therapy following anti-PD-1 mAb alone also reversed the resistance in our mouse experiments. From these findings, PD-1^+ T_{reg} cell infiltration and T_{reg} cell antigens may be predictive biomarkers for combination therapy. However, the strong autofluorescence made it challenging to evaluate PD-1

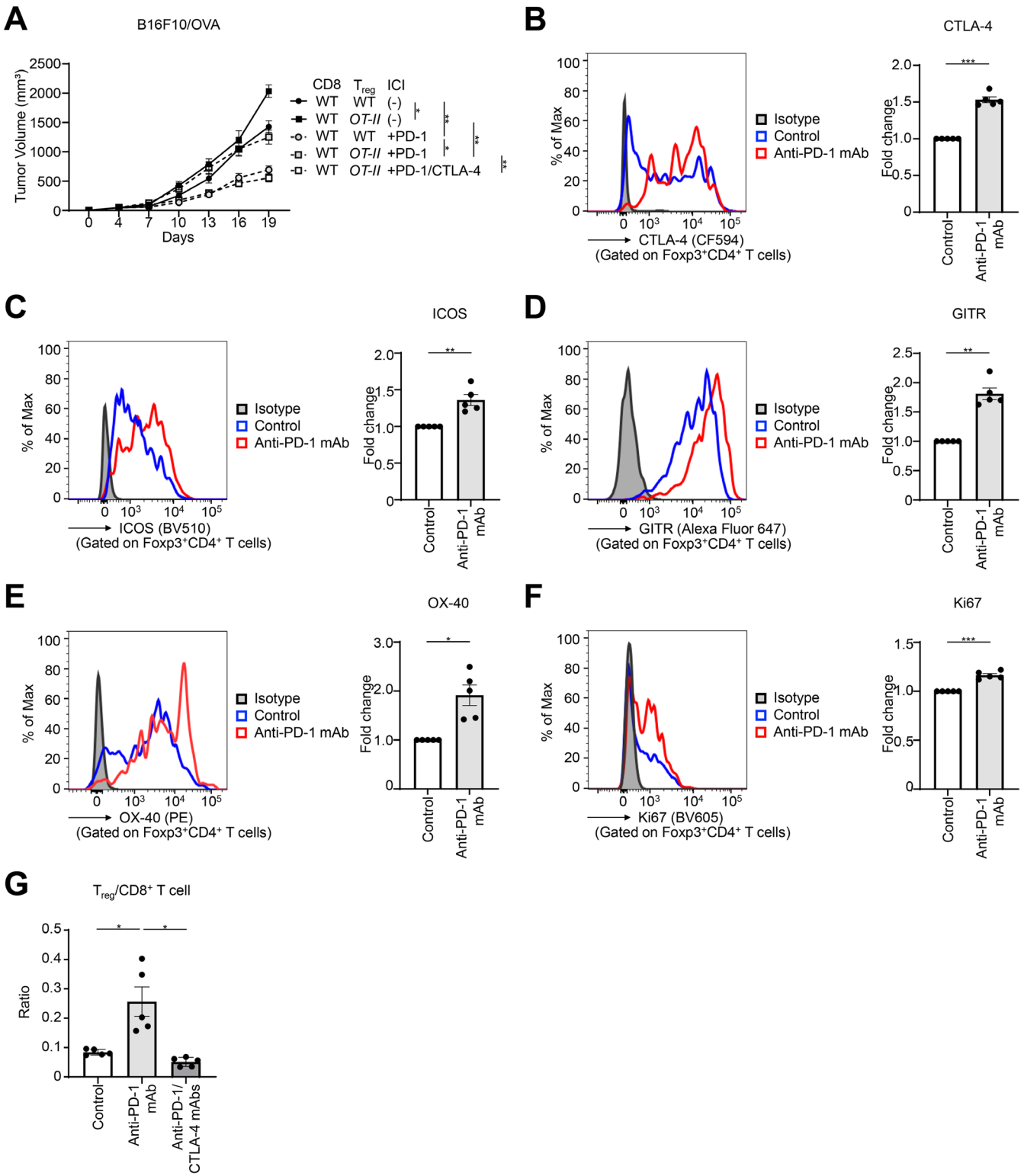

FIGURE 6 | Tumor growth and analyses of tumor-infiltrating OT-II T_{reg} cells in adoptive T-cell transfer models treated with PD-1 and/or CTLA-4 blockade. In vivo experiments were performed as described in Figure 5A. (A) B16F10/OVA tumor growth curves in B6 SCID mice treated with adoptive T-cell transfer combined with PD-1 and/or CTLA-4 blockade. (B–F) CTLA-4 (B), ICOS (C), GITR (D), OX-40 (E), and Ki67 (F) expression in tumor-infiltrating OT-II T_{reg} cells treated with or without PD-1 blockade. Representative flow cytometry staining (left) and summaries (right) are shown ($n = 5$). (G) T_{reg}/$CD8^+$ T-cell ratios in TILs treated with or without PD-1 and/or CTLA-4 blockade. Summary is shown ($n = 5$). $^*p < 0.05$; $^{**}p < 0.01$; $^{***}p < 0.001$; bars, mean; error bars, SEM.

expression in T_{reg} cells from our melanoma samples using multiplex fluorescent immunostaining. To validate our findings, larger prospective studies using fresh TILs are warranted.

In summary, we demonstrated the importance of the antigenicity of T_{reg} cells on PD-1 expression in T_{reg} cells. Tumors with high antigenicity for T_{reg} cells were resistant to PD-1 blockade

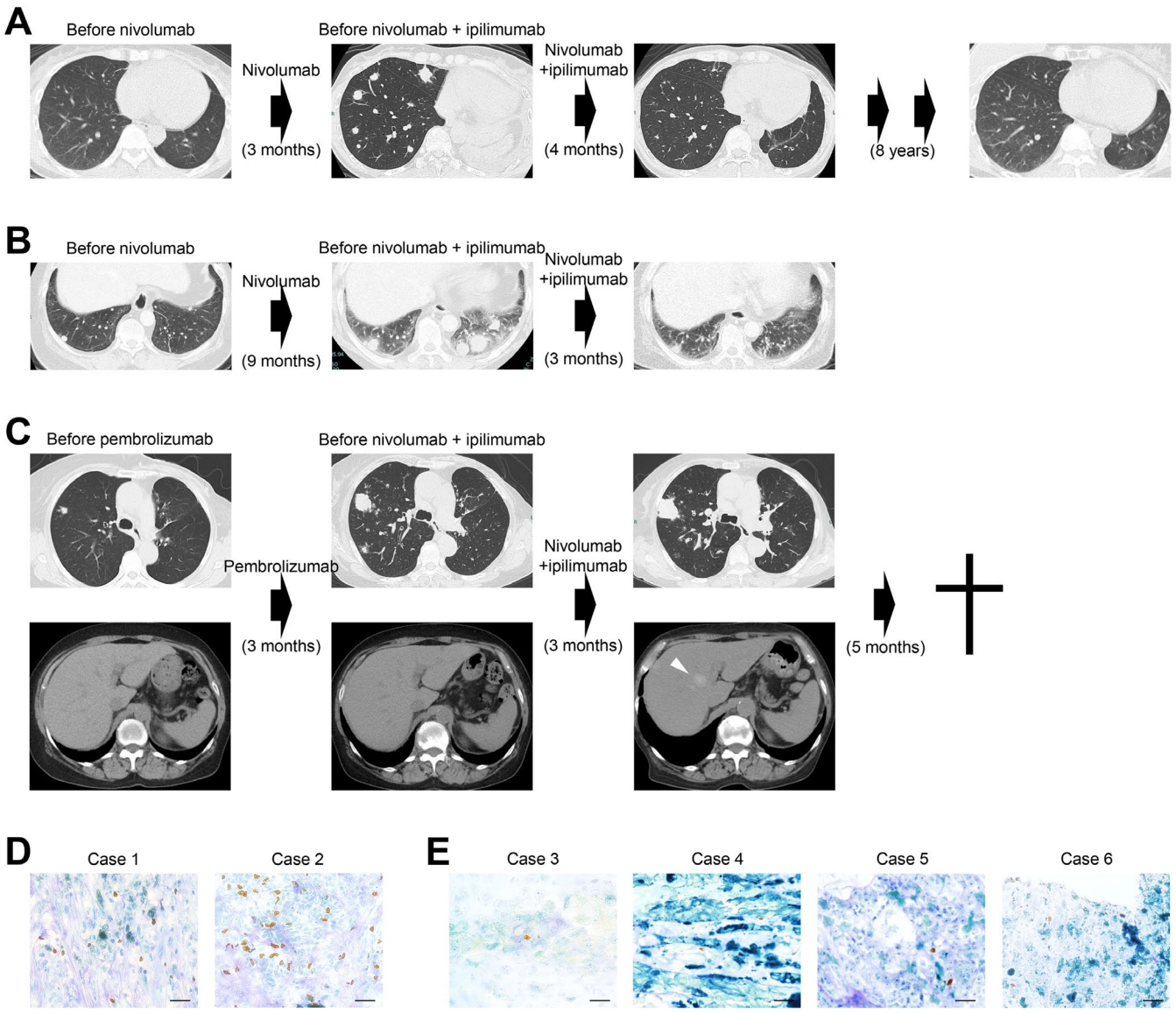

FIGURE 7 | Clinical courses and IHC. (A) Computed tomography imaging of case 1 who responded to combination with anti-PD-1 and anti-CTLA-4 mAbs sequentially after primary resistance to an anti-PD-1 mAb. She experienced progressive disease in lung metastases 3 months after first line nivolumab monotherapy at the first evaluation. Subsequently, she received combination therapy with ipilimumab as second line treatment. Four months later, tumors dramatically responded to the combination therapy. She achieved complete response for more than 8 years even without any therapies. (B) Computed tomography imaging of case 2 who responded to combination with anti-PD-1 and anti-CTLA-4 mAbs sequentially after primary resistance to an anti-PD-1 mAb. He experienced progressive disease in lung metastases 4 months after first line nivolumab monotherapy at the first evaluation, but continued monotherapy for 9 months without any tumor shrinkage. However, lung metastases further exacerbated. Subsequently, he received combination therapy with ipilimumab as second line treatment. Three months later, tumors dramatically responded to the combination therapy. (C) Computed tomography imaging of case 6 who failed to respond to combination with anti-PD-1 and anti-CTLA-4 mAbs sequentially after primary resistance to an anti-PD-1 mAb. She experienced progressive disease in lung metastases 3 months after 1st line pembrolizumab monotherapy at the first evaluation. Subsequently, she received combination therapy of nivolumab and ipilimumab as second line treatment. Three months later, lung tumor size increased and new liver metastases appeared (an arrow) and the treatment was discontinued. She died 5 months after the discontinuation. (D, E) immunohistochemistry (IHC) of cases 1, 2 (D) and 3–6 (E). Formalin fixed paraffin embedded (FFPE) samples before the initiation of anti-PD-1 mAb monotherapy were stained with an anti-Foxp3 mAb and representative staining are shown. Scale bars, 20 μm.

by PD-1$^+$ T_{reg} cells. Additionally, resistant tumors responded to the combination therapy with anti-CTLA-4 mAbs. We propose that the high antigenicity of T_{reg} cells confers resistance to PD-1 blockade therapy via high PD-1 expression in T_{reg} cells, which can be overcome by combination therapy with anti-CTLA-4 mAbs. PD-1$^+$ T_{reg} cell infiltration and T_{reg} cell antigens may be predictive biomarkers for combination therapies.

Author Contributions

Hiroaki Matsuura: data curation, formal analysis, writing – original draft. **Takamasa Ishino:** data curation, formal analysis. **Toshifumi Ninomiya:** data curation, formal analysis. **Kiichiro Ninomiya:** conceptualization, project administration, resources.

Kota Tachibana: resources. **Akiko Honobe-Tabuchi:** resources. **Yoshinori Muto:** resources. **Takashi Inozume:** resources. **Youki Ueda:** data curation, formal analysis. **Kadoaki Ohashi:** supervision. **Yoshinobu Maeda:** project administration, supervision. **Joji Nagasaki:** data curation, formal analysis. **Yosuke Togashi:** conceptualization, data curation, formal analysis, project administration, writing – original draft.

Acknowledgments

We thank Mr. Y. Kurihara, Ms. M. Iwado, Ms. Y. Nishimori, Ms. R. Inukai, and Ms. M. Konishi for technical and administrative assistance.

Ethics Statement

The protocols of this study were approved by the appropriate institutional review boards and ethics committees at Okayama University Hospital (2203-025 and 2017-029) and Yamanashi University Hospital (1795). This study was conducted in accordance with the Declaration of Helsinki.

Registry and the Registration No. of the study/trial: N/A.

Animal Studies: All animal experiments were reviewed and approved by the Institutional Animal Care and Research Advisory Committee, Okayama University.

Consent

All informed consent was obtained in the form of opt-out on the website.

Conflicts of Interest

K. Ninomiya received honoraria from Ono Pharmaceutical, Bristol-Myers Squibb, Chugai Pharmaceutical, AstraZeneca, Daiichi-Sankyo, MSD, Kyowa Kirin, Lilly, Takeda Pharmaceutical, Nippon Kayaku, Pfizer, Janssen Pharmaceutical, Boehringer Ingelheim, Taiho Pharmaceutical, Amgen, Elekta, and CareNet outside this study. T. Inozume received honoraria from Ono Pharmaceutical, Bristol-Myers Squibb, and MSD; and research grants from Maruho, Taiho, Daiichi-Sankyo, Torii, and Sun Pharma outside this study. K. Ohashi received honoraria from Boehringer Ingelheim, Chugai Pharmaceutical, Pfizer, Eli Lilly, Nippon Kayaku, KYOWA KIRIN, AstraZeneca, MSD, Novartis, Insmed, and Elekta; and research grants from Boehringer Ingelheim and Chugai Pharmaceutical outside of this study. Y. Togashi received honoraria from Ono Pharmaceutical, Bristol-Myers Squibb, Chugai Pharmaceutical, AstraZeneca, Eisai, and MSD; and research grants from Ono Pharmaceutical, Bristol-Myers Squibb, Daiichi-Sankyo, Janssen Pharmaceutical, AstraZeneca, KOTAI Biotechnologies Inc., and KORTUC outside this study, is the Associate Editor of Cancer Science. All the other authors declare that they have no competing financial interests.

References

1. J. R. Brahmer, S. S. Tykodi, L. Q. Chow, et al., "Safety and Activity of Anti-PD-L1 Antibody in Patients With Advanced Cancer," *New England Journal of Medicine* 366 (2012): 2455–2465.

2. S. L. Topalian, F. S. Hodi, J. R. Brahmer, et al., "Safety, Activity, and Immune Correlates of Anti-PD-1 Antibody in Cancer," *New England Journal of Medicine* 366 (2012): 2443–2454.

3. Y. Doki, J. A. Ajani, K. Kato, et al., "Nivolumab Combination Therapy in Advanced Esophageal Squamous-Cell Carcinoma," *New England Journal of Medicine* 386 (2022): 449–462.

4. M. D. Hellmann, L. Paz-Ares, R. Bernabe Caro, et al., "Nivolumab Plus Ipilimumab in Advanced Non-Small-Cell Lung Cancer," *New England Journal of Medicine* 381 (2019): 2020–2031.

5. P. Baas, A. Scherpereel, A. K. Nowak, et al., "First-Line Nivolumab Plus Ipilimumab in Unresectable Malignant Pleural Mesothelioma (CheckMate 743): A Multicentre, Randomised, Open-Label, Phase 3 Trial," *Lancet* 397 (2021): 375–386.

6. R. J. Motzer, N. M. Tannir, D. F. McDermott, et al., "Nivolumab Plus Ipilimumab Versus Sunitinib in Advanced Renal-Cell Carcinoma," *New England Journal of Medicine* 378 (2018): 1277–1290.

7. J. Larkin, V. Chiarion-Sileni, R. Gonzalez, et al., "Combined Nivolumab and Ipilimumab or Monotherapy in Untreated Melanoma," *New England Journal of Medicine* 373 (2015): 23–34.

8. M. J. Overman, S. Lonardi, K. Y. M. Wong, et al., "Durable Clinical Benefit With Nivolumab Plus Ipilimumab in DNA Mismatch Repair-Deficient/Microsatellite Instability-High Metastatic Colorectal Cancer," *Journal of Clinical Oncology* 36 (2018): 773–779.

9. R. K. Kelley, B. Sangro, W. Harris, et al., "Safety, Efficacy, and Pharmacodynamics of Tremelimumab Plus Durvalumab for Patients With Unresectable Hepatocellular Carcinoma: Randomized Expansion of a Phase I/II Study," *Journal of Clinical Oncology* 39 (2021): 2991–3001.

10. Y. Shiraishi, Y. Sekino, H. Horinouchi, Y. Ohe, and I. Okamoto, "High Incidence of Cytokine Release Syndrome in Patients With Advanced NSCLC Treated With Nivolumab Plus Ipilimumab," *Annals of Oncology* 34 (2023): 1064–1065.

11. Y. Shiraishi, S. Nomura, S. Sugawara, et al., "Comparison of Platinum Combination Chemotherapy Plus Pembrolizumab Versus Platinum Combination Chemotherapy Plus Nivolumab–Ipilimumab for Treatment-Naive Advanced Non-small-Cell Lung Cancer in Japan (JCOG2007): An Open-Label, Multicentre, Randomised, Phase 3 Trial," *Lancet Respiratory Medicine* 12 (2024): 877–887.

12. S. Sakaguchi, N. Sakaguchi, M. Asano, M. Itoh, and M. Toda, "Immunologic Self-Tolerance Maintained by Activated T Cells Expressing IL-2 Receptor Alpha-Chains (CD25). Breakdown of a Single Mechanism of Self-Tolerance Causes Various Autoimmune Diseases," *Journal of Immunology* 155 (1995): 1151–1164.

13. Y. Togashi, K. Shitara, and H. Nishikawa, "Regulatory T Cells in Cancer Immunosuppression–Implications for Anticancer Therapy," *Nature Reviews. Clinical Oncology* 16 (2019): 356–371.

14. S. Onizuka, I. Tawara, J. Shimizu, S. Sakaguchi, T. Fujita, and E. Nakayama, "Tumor Rejection by In Vivo Administration of Anti-CD25 (Interleukin-2 Receptor Alpha) Monoclonal Antibody," *Cancer Research* 59 (1999): 3128–3133.

15. J. Shimizu, S. Yamazaki, and S. Sakaguchi, "Induction of Tumor Immunity by Removing $CD25^+CD4^+$ T Cells: A Common Basis Between Tumor Immunity and Autoimmunity," *Journal of Immunology* 163 (1999): 5211–5218.

16. S. Kumagai, Y. Togashi, T. Kamada, et al., "The PD-1 Expression Balance Between Effector and Regulatory T Cells Predicts the Clinical Efficacy of PD-1 Blockade Therapies," *Nature Immunology* 21 (2020): 1346–1358.

17. T. Kamada, Y. Togashi, C. Tay, et al., "$PD\text{-}1^+$ Regulatory T Cells Amplified by PD-1 Blockade Promote Hyperprogression of Cancer," *Proceedings of the National Academy of Sciences of the United States of America* 116 (2019): 9999–10008.

18. M. van Gulijk, A. van Krimpen, S. Schetters, et al., "PD-L1 Checkpoint Blockade Promotes Regulatory T Cell Activity That Underlies Therapy Resistance," *Science Immunology* 8 (2023): eabn6173.

19. Y. Agata, A. Kawasaki, H. Nishimura, et al., "Expression of the PD-1 Antigen on the Surface of Stimulated Mouse T and B Lymphocytes," *International Immunology* 8 (1996): 765–772.

20. B. Reynisson, B. Alvarez, S. Paul, B. Peters, and M. Nielsen, "NetMHCpan-4.1 and NetMHCIIpan-4.0: Improved Predictions of MHC Antigen Presentation by Concurrent Motif Deconvolution and Integration

of MS MHC Eluted Ligand Data," *Nucleic Acids Research* 48 (2020): W449–W454.

21. B. Reynisson, C. Barra, S. Kaabinejadian, W. H. Hildebrand, B. Peters, and M. Nielsen, "Improved Prediction of MHC II Antigen Presentation Through Integration and Motif Deconvolution of Mass Spectrometry MHC Eluted Ligand Data," *Journal of Proteome Research* 19 (2020): 2304–2315.

22. M. W. Moore, F. R. Carbone, and M. J. Bevan, "Introduction of Soluble Protein Into the Class I Pathway of Antigen Processing and Presentation," *Cell* 54 (1988): 777–785.

23. J. M. Robertson, P. E. Jensen, and B. D. Evavold, "DO11.10 and OT-II T Cells Recognize a C-Terminal Ovalbumin 323-339 Epitope," *Journal of Immunology* 164 (2000): 4706–4712.

24. S. S. Diebold, M. Cotten, N. Koch, and M. Zenke, "MHC Class II Presentation of Endogenously Expressed Antigens by Transfected Dendritic Cells," *Gene Therapy* 8 (2001): 487–493.

25. J. P. Morgenstern and H. Land, "Advanced Mammalian Gene Transfer: High Titre Retroviral Vectors With Multiple Drug Selection Markers and a Complementary Helper-Free Packaging Cell Line," *Nucleic Acids Research* 18 (1990): 3587–3596.

26. D. Q. Tran, H. Ramsey, and E. M. Shevach, "Induction of FOXP3 Expression in Naive Human CD4+FOXP3 T Cells by T-Cell Receptor Stimulation Is Transforming Growth Factor-Beta Dependent but Does Not Confer a Regulatory Phenotype," *Blood* 110 (2007): 2983–2990.

27. M. Miyara, Y. Yoshioka, A. Kitoh, et al., "Functional Delineation and Differentiation Dynamics of Human CD4+ T Cells Expressing the FoxP3 Transcription Factor," *Immunity* 30 (2009): 899–911.

28. Y. L. Cho, M. Flossdorf, L. Kretschmer, T. Höfer, D. H. Busch, and V. R. Buchholz, "TCR Signal Quality Modulates Fate Decisions of Single CD4+ T Cells in a Probabilistic Manner," *Cell Reports* 20 (2017): 806–818.

29. K. M. Jeltsch, D. Hu, S. Brenner, et al., "Cleavage of Roquin and Regnase-1 by the Paracaspase MALT1 Releases Their Cooperatively Repressed Targets to Promote T(H)17 Differentiation," *Nature Immunology* 15 (2014): 1079–1089.

30. T. Yokosuka, M. Takamatsu, W. Kobayashi-Imanishi, A. Hashimoto-Tane, M. Azuma, and T. Saito, "Programmed Cell Death 1 Forms Negative Costimulatory Microclusters That Directly Inhibit T Cell Receptor Signaling by Recruiting Phosphatase SHP2," *Journal of Experimental Medicine* 209 (2012): 1201–1217.

31. S. Kumagai, S. Koyama, K. Itahashi, et al., "Lactic Acid Promotes PD-1 Expression in Regulatory T Cells in Highly Glycolytic Tumor Microenvironments," *Cancer Cell* 40 (2022): 201–218.e9.

32. H. Takaba and H. Takayanagi, "The Mechanisms of T Cell Selection in the Thymus," *Trends in Immunology* 38 (2017): 805–816.

33. M. S. Jordan, A. Boesteanu, A. J. Reed, et al., "Thymic Selection of $CD4^+CD25^+$ Regulatory T Cells Induced by an Agonist Self-Peptide," *Nature Immunology* 2 (2001): 301–306.

34. I. Apostolou, A. Sarukhan, L. Klein, and H. von Boehmer, "Origin of Regulatory T Cells With Known Specificity for Antigen," *Nature Immunology* 3 (2002): 756–763.

35. J. R. Killebrew, N. Perdue, A. Kwan, A. M. Thornton, E. M. Shevach, and D. J. Campbell, "A Self-Reactive TCR Drives the Development of Foxp3+ Regulatory T Cells That Prevent Autoimmune Disease," *Journal of Immunology* 187 (2011): 861–869.

36. J. Cabarrocas, C. Cassan, F. Magnusson, et al., "$Foxp3^+$ $CD25^+$ Regulatory T Cells Specific for a Neo-Self-Antigen Develop at the Double-Positive Thymic Stage," *Proceedings of the National Academy of Sciences of the United States of America* 103 (2006): 8453–8458.

37. X. Tai, A. Indart, M. Rojano, et al., "How Autoreactive Thymocytes Differentiate Into Regulatory Versus Effector CD4," *Nature Immunology* 24 (2023): 637–651.

38. M. Ahmadzadeh, A. Pasetto, L. Jia, et al., "Tumor-Infiltrating Human $CD4^+$ Regulatory T Cells Display a Distinct TCR Repertoire and Exhibit Tumor and Neoantigen Reactivity," *Science Immunology* 4 (2019): 4.

39. G. Oliveira, K. Stromhaug, N. Cieri, et al., "Landscape of Helper and Regulatory Antitumour $CD4^+$ T Cells in Melanoma," *Nature* 605 (2022): 532–538.

40. T. R. Simpson, F. Li, W. Montalvo-Ortiz, et al., "Fc-Dependent Depletion of Tumor-Infiltrating Regulatory T Cells Co-Defines the Efficacy of Anti-CTLA-4 Therapy Against Melanoma," *Journal of Experimental Medicine* 210 (2013): 1695–1710.

41. D. Ha, A. Tanaka, T. Kibayashi, et al., "Differential Control of Human Treg and Effector T Cells in Tumor Immunity by Fc-Engineered Anti-CTLA-4 Antibody," *Proceedings of the National Academy of Sciences of the United States of America* 116 (2019): 609–618.

42. M. J. Selby, J. J. Engelhardt, M. Quigley, et al., "Anti-CTLA-4 Antibodies of IgG2a Isotype Enhance Antitumor Activity Through Reduction of Intratumoral Regulatory T Cells," *Cancer Immunology Research* 1 (2013): 32–42.

43. E. Romano, M. Kusio-Kobialka, P. G. Foukas, et al., "Ipilimumab-Dependent Cell-Mediated Cytotoxicity of Regulatory T Cells Ex Vivo by Nonclassical Monocytes in Melanoma Patients," *Proceedings of the National Academy of Sciences of the United States of America* 112 (2015): 6140–6145.

44. T. Watanabe, T. Ishino, Y. Ueda, et al., "Activated CTLA-4-Independent Immunosuppression of Treg Cells Disturbs CTLA-4 Blockade-Mediated Antitumor Immunity," *Cancer Science* 114 (2023): 1859–1870.

Supporting Information

Additional supporting information can be found online in the Supporting Information section.